Mechanics of debonding in FRP-plated RC beams

Proceedings of the Institution of Civil Engineers
Structures and Buildings 162
October 2009 Issue SB5
Pages 335–345
doi: 10.1680/stbu.2009.162.5.335

Paper 800068
Received 12/09/2008
Accepted 24/03/2009

Keywords: beams & girders/ concrete structures/rehabilitation, reclamation & renovation

J. G. Teng
Department of Civil and Structural Engineering, The Hong Kong Polytechnic University, Hong Kong, China

J. F. Chen
Institute for Infrastructure and Environment, Joint Research Institute for Civil and Environmental Engineering, School of Engineering, The University of Edinburgh, Edinburgh, UK

ice
Institution of Civil Engineers

Mechanics of debonding in FRP-plated RC beams

J. G. Teng BEng, PhD, FHKIE, FIIFC and J. F. Chen BEng, MSc, PhD, FIIFC

Both the flexural and shear strengths of reinforced concrete (RC) beams can be substantially increased using externally bonded fibre-reinforced polymer (FRP) reinforcement in the forms of sheets/strips/plates (all referred to as plates for brevity). Failures of such FRP-plated RC beams often occur by debonding of the FRP plate from the RC beam in a number of distinct modes. This paper provides a summary of the current understanding of the mechanics of debonding failures in FRP-plated RC beams largely based on the research of the authors and their co-workers. A systematic classification of possible debonding failure modes is presented following a brief outline of the common strengthening methods. The interfacial stresses and bond behaviour between FRP and concrete are then discussed before the mechanisms and processes of debonding failures are examined. Furthermore, advanced strength models for the key debonding failure modes are presented. The paper concludes with a brief discussion of future research needs.

1. INTRODUCTION

Strengthening reinforced concrete (RC) structures with externally bonded fibre-reinforced polymer (FRP) composites has become a popular technique in recent years.[1,2] The technique may be used to enhance the load-carrying capacities of RC beams, slabs and columns as well as the ductility of RC columns through lateral confinement.

Both the flexural and shear strengths of RC beams can be substantially increased using externally bonded FRP reinforcement in the forms of sheets/strips/plates (all referred to as plates hereafter unless specific differentiation becomes necessary). Failures of such FRP-strengthened RC beams (also referred to as FRP-plated RC beams) often occur by debonding of the FRP plate from the RC beam in a number of modes. Despite numerous theoretical and experimental studies, current knowledge of the mechanics of such debonding failures is still far from complete.

The current paper provides a summary of the authors' understanding of the subject largely based on the research of the authors and their co-workers. Following a brief outline of the common methods for the flexural and shear strengthening of RC beams using FRP composites, the paper examines the following issues in some detail

(*a*) interfacial stresses and bond behaviour between FRP and concrete
(*b*) classification of debonding failure modes
(*c*) mechanisms and processes of debonding failures
(*d*) theoretical models for debonding failures.

The paper concludes with a brief discussion of future research needs. For simplicity, all discussions in this paper are presented with explicit reference to a simply supported beam (Figure 1), but the information is also generally applicable to indeterminate beams by treating each segment between two points of inflection as a simply supported beam.

2. COMMON METHODS FOR FLEXURAL AND SHEAR STRENGTHENING

2.1. Flexural strengthening

FRP flexural strengthening of RC beams is commonly achieved by bonding an FRP plate to its soffit (Figure 1). The FRP plate may be a prefabricated (e.g. pultruded) plate or a plate formed on site in a wet lay-up process.[1] The strengthening plate is most commonly unstressed. However, the plate may be pre-tensioned to achieve a fuller use of the tensile strength of the FRP plate, to obtain a significant increase in the stiffness of the beam or to reduce the widths of cracks in the beam. Anchors such as U jackets[3] and fibre anchors[4] may be provided to reduce the risk of debonding failures. For simplicity of discussion, this paper is focused on RC beams strengthened with unstressed plates without additional anchors.

Existing research has shown that RC beams bonded with a tension face plate often fail by debonding of the FRP plate from the beam in one of several possible modes.[1,4–8] Despite extensive existing research, there is still considerable uncertainty regarding many aspects of debonding failures, including the classification of debonding failure modes.

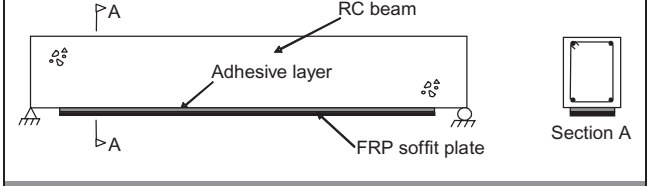

Figure 1. RC beam with an FRP plate bonded to its soffit

2.2. Shear strengthening

The shear capacity of an RC beam can also be effectively enhanced using externally bonded FRP reinforcement in various forms (Figure 2). These include bonding FRP to the sides of a beam only (side bonding), bonding FRP U jackets to both the sides and the soffit (U jacketing) and wrapping FRP around the whole cross-section of a beam (complete wrapping). Both FRP strips and continuous sheets have been used. The fibres may be orientated in such directions as to best control shear cracks. Furthermore, fibres may be arranged at two different directions to satisfy the requirement of shear strengthening in both directions if the shear forces in a beam may be reversed under reversed cyclic loading and earthquake attacks. The use of fibres in two directions can obviously be beneficial to shear resistance, even if strengthening for reversed cyclic loading is not required. In this sense, FRPs with fibres in three directions (e.g. $0^o/60^o/120^o$) may also be used. The combination of different bonding configurations, fibre orientations and fibre distributions can result in many different strengthening schemes (Figure 2). For both side bonding and U jacketing, mechanical anchors may be required at the free ends of FRP strips/sheets.

Experimental evidence shows that debonding of FRP from concrete occurs in almost all RC beams shear-strengthened with FRP,[9–11] although in the case of complete wraps, debonding does not directly control the ultimate load because debonded FRP wraps can continue to carry forces.[11]

3. INTERFACIAL STRESSES

In an FRP-plated beam, high interfacial stresses exist between the FRP plate and the RC beam near the plate ends.[12] The two main components of interfacial stresses are the interfacial shear stress τ and the interfacial normal stress σ_y (Figure 3). These high interfacial stresses play an important role in some of the debonding failure modes including the modes of concrete cover separation and plate end interfacial debonding which are discussed in more detail later. Obviously, higher interfacial stresses mean a greater risk of debonding failure at a plate end, although it is difficult to relate the magnitude of interfacial stresses to debonding failure in a simple direct manner.

Many analytical solutions have been presented for interfacial stresses in FRP-plated beams, with most of them being

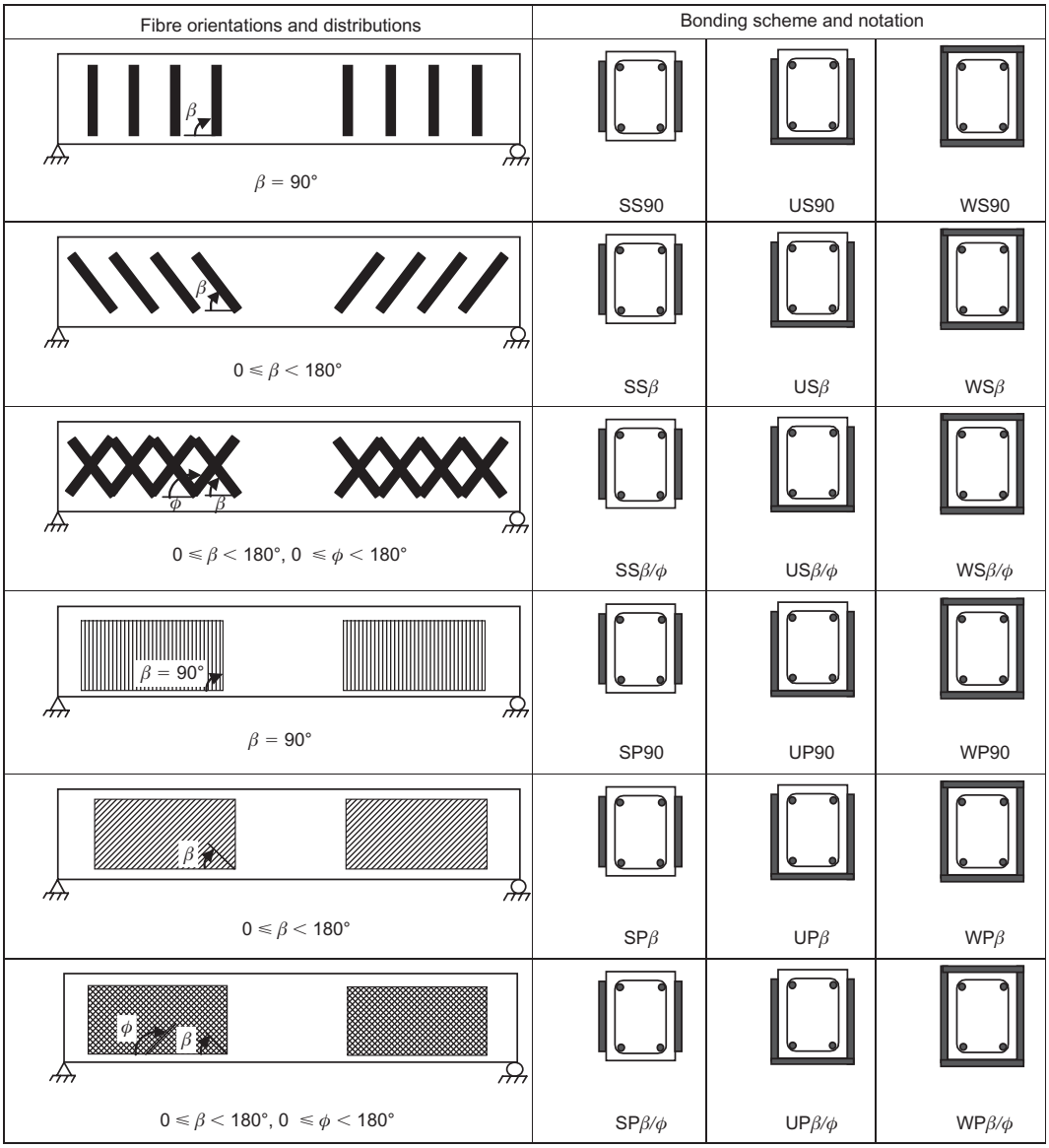

Figure 2. Shear strengthening schemes for RC beams using externally bonded FRP reinforcement

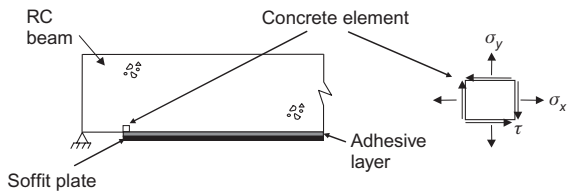

Figure 3. Stresses acting on a concrete element adjacent to the plate end

concerned with the linear elastic analysis of FRP-plated beams. A simple analytical solution for interfacial stresses in such beams has been presented by Smith and Teng.[12] Interfacial stresses predicted by finite element analysis show a much more complex picture,[13] but results from the simple analytical solution of Smith and Teng,[12] as shown in Figure 4 for a typical case, are sufficient to illustrate the stress concentration phenomenon in the vicinity of the plate end. Figure 4 shows that near the plate end, both the interfacial shear and normal stresses increase rapidly. For a given simply supported beam under transverse loading, the magnitudes of these stresses increase with the distance between the support and the plate end, with both the elastic modulus and the thickness of the plate, and with the elastic modulus of the adhesive layer, but decrease as the thickness of the adhesive layer increases.[12–15]

4. BOND BEHAVIOUR

4.1. General

A good understanding of the bond behaviour between the FRP plate and the substrate concrete is of great importance for understanding and predicting debonding failures in FRP-plated RC beams. Bond behaviour between FRP and concrete has been widely studied experimentally using simple pull-off tests or using theoretical/finite element models.[16–18] Figure 5 shows the schematic diagram of the widely used simple pull-off test. A more detailed discussion on the bond strength test methods can be found in Chen *et al.*[19] The discussions presented below use the simple pull-off test (Figure 5) as the reference case.

4.2. Bond strength

The ultimate tensile force that can be resisted by the FRP plate in a simple puff-off test before the FRP plate debonds from the concrete prism is referred to as the ultimate load or the bond strength. The bond strength is defined herein using the tensile force (or the tensile stress) in the plate instead of the average interfacial shear stress because the latter can be conceptually

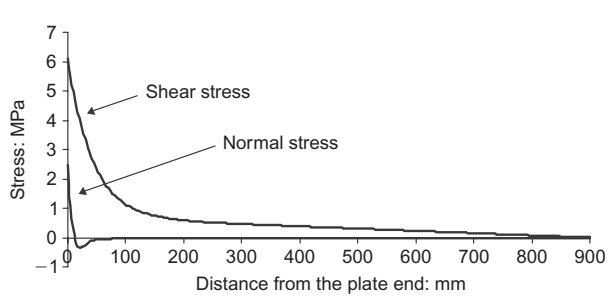

Figure 4. Typical interfacial shear and normal stress distributions

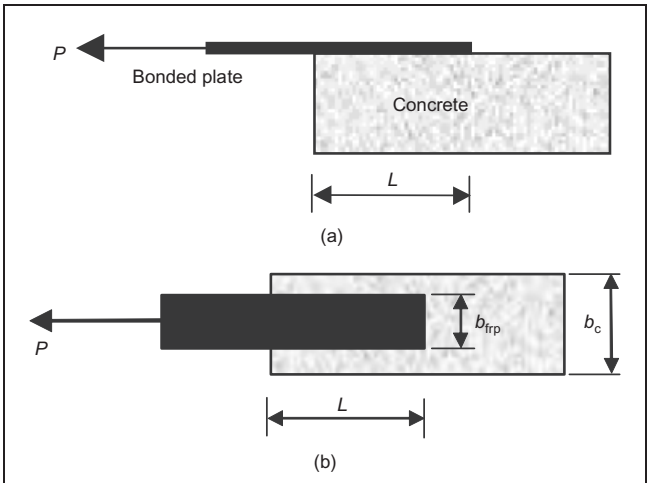

Figure 5. Schematic diagram of a simple pull-off test: (a) elevation; (b) plan

misleading. Existing research has shown conclusively[16–18] that the ultimate load of a pull-off test initially increases as the bond length increases, but when the bond length reaches a threshold value, any further increase in the bond length does not lead to a further increase in the ultimate load. Therefore, when a long bond length is used, only part of the bond length is mobilised in resisting the ultimate load, so the use of an average interfacial stress referring to the entire bond length is inappropriate. This threshold value of the bond length is referred to as the effective bond length.[16]

The fact that the bond strength cannot increase further once the bond length exceeds the effective bond length means that the ultimate tensile strength of an FRP plate may never be reached in a pull-off test, however long the bond length would be. A longer bond length, however, can improve the ductility of the failure process.[17,18] In most tests on FRP-to-concrete bonded joints, failure occurred by crack propagation in the concrete adjacent to the adhesive-to-concrete interface, starting from the loaded end of the plate. This phenomenon is substantially different from the bond behaviour of internal reinforcement, for which a bond length can always be designed for its full tensile strength if an adequate concrete cover can be provided.

Many theoretical models have been developed to predict the bond strength of FRP-to-concrete bonded joints.[16,20] Among the existing bond strength models, the model developed by Chen and Teng[16] has recently been confirmed by Lu *et al.*[20] to provide the most accurate predictions of test results. Chen and Teng's[16] bond strength model predicts that the stress in the bonded plate in MPa, to cause debonding failure in a simple pull-off test is given by

$$\sigma_p = \alpha \beta_w \beta_L \sqrt{\frac{E_{frp}\sqrt{f'_c}}{t_{frp}}} \quad (1)$$

where the FRP-to-concrete width ratio factor is given by

$$\beta_w = \sqrt{\frac{2 - b_{frp}/b_c}{1 + b_{frp}/b_c}} \quad (2)$$

and the bond length factor is given by

$$\beta_L = \begin{cases} 1 & \text{if } L \geqslant L_e \\ \sin\left(\dfrac{\pi L}{2L_e}\right) & \text{if } L < L_e \end{cases} \quad (3)$$

with the effective bond length being defined by

$$L_e = \sqrt{\frac{E_{frp}\, t_{frp}}{\sqrt{f'_c}}} \quad (4)$$

in which E_{frp}, t_{frp} and b_{frp} are the elastic modulus (MPa), thickness (mm) and width (mm) of the FRP plate respectively, f'_c and b_c are the concrete cylinder compressive strength (MPa) and width (mm) of the concrete prism respectively, and L is the bond length (mm). A value of 0·427 for α was found by Chen and Teng[16] to provide the best fit of the test data gathered by them, while a value of 0·315 was shown by them to provide a 95 percentile lower bound which is suitable for use in ultimate limit state design.

4.3. Bond–slip behaviour

For the accurate prediction of debonding failures in FRP-plated RC beams, the bond–slip behaviour of FRP-to-concrete interfaces needs to be understood and accurately modelled. Both experimental and theoretical studies have been undertaken on the FRP-to-concrete bond slip behaviour.[18,21] Lu *et al.*[20] conducted a thorough review of bond–slip models and then proposed a set of three bond–slip models of different levels of sophistication based on a combination of experimental data and meso-scale finite element simulations: the precise model, the simplified model and the bilinear model (Figure 6). The bilinear model is the easiest to implement, without a significant loss of accuracy compared with the precise and simplified models and is defined by the following equations

$$\tau = \tau_{max}\frac{s}{s_0} \quad \text{if } s \leqslant s_0 \quad (5a)$$

$$\tau = \tau_{max}\frac{s_f - s}{s_f - s_0} \quad \text{if } s_0 < s \leqslant s_f \quad (5b)$$

$$\tau = 0 \quad \text{if } s > s_f \quad (5c)$$

where

$$s_f = 2G_f/\tau_{max} \quad (6)$$

In the above equations, $\tau_{max} = 1{\cdot}5\beta_w f_t$, $s_0 = 0{\cdot}0195\beta_w f_t$, $G_f = 0{\cdot}308\beta_w^2\sqrt{f_t}$, s (mm) is the local slip, s_0 (mm) the local slip at the maximum local bond stress τ_{max} (MPa), and s_f (mm) the local slip when the local bond stress τ (MPa) reduces to zero. The interfacial fracture energy is denoted by G_f (MPa mm), and f_t is the concrete tensile strength (MPa). It should be noted that in Lu *et al.*'s original model,[20] a slightly different expression was proposed for the width ratio factor β_w, but the expression given by Equation 2 can be used in the above equations without any significant loss of accuracy.

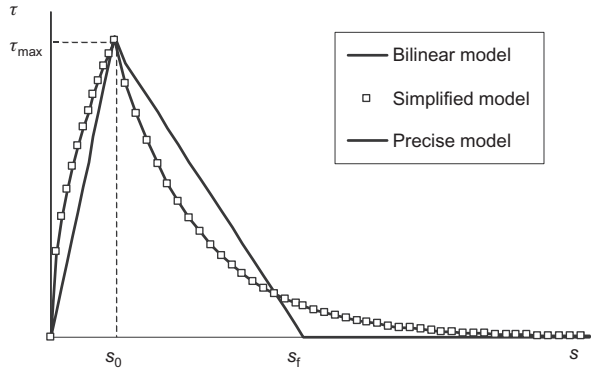

Figure 6. Lu *et al.*'s bond–slip models: (a) FRP rupture; (b) crushing of compressive concrete

5. DEBONDING FAILURE MODES OF FLEXURALLY STRENGTHENED RC BEAMS

5.1. Classification of failure modes

A number of distinct failure modes of FRP-plated RC beams have been observed in numerous experimental studies.[1,8,22,23] A schematic representation of these failure modes is shown in Figures 7 and 8. Failure of an FRP-plated RC beam may be by the flexural failure of the critical section (Figure 7) or by debonding of the FRP plate from the RC beam (Figure 8). In the former type of failure, the composite action between the bonded plate and the RC beam is maintained up to failure, while the latter type of failure involves a loss of this composite action. Debonding failures generally occur in the concrete, which is also assumed in the strength models presented in this paper. This is because, with the strong adhesives currently available and with appropriate surface preparation for the concrete substrate, debonding failures along the physical interfaces between the adhesive and the concrete and between the adhesive and the FRP plate are generally not critical.

Debonding may initiate at a flexural or flexural-shear crack in the high moment region and then propagates towards one of the plate ends (Figure 8(a)). This debonding failure mode is commonly referred to as intermediate crack (IC) induced interfacial debonding (or simply IC debonding).[1,7,24,25] Debonding may also occur at or near a plate end (i.e. plate end debonding failures) in four different modes

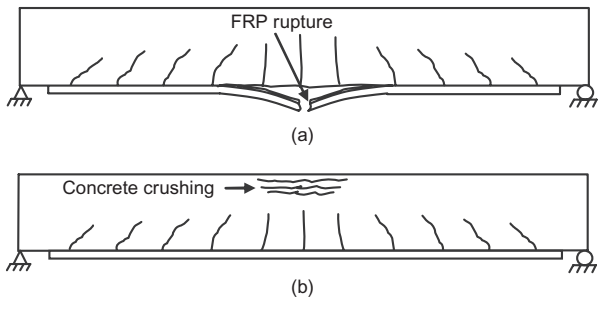

Figure 7. Conventional flexural failure modes of an FRP-plated RC beam

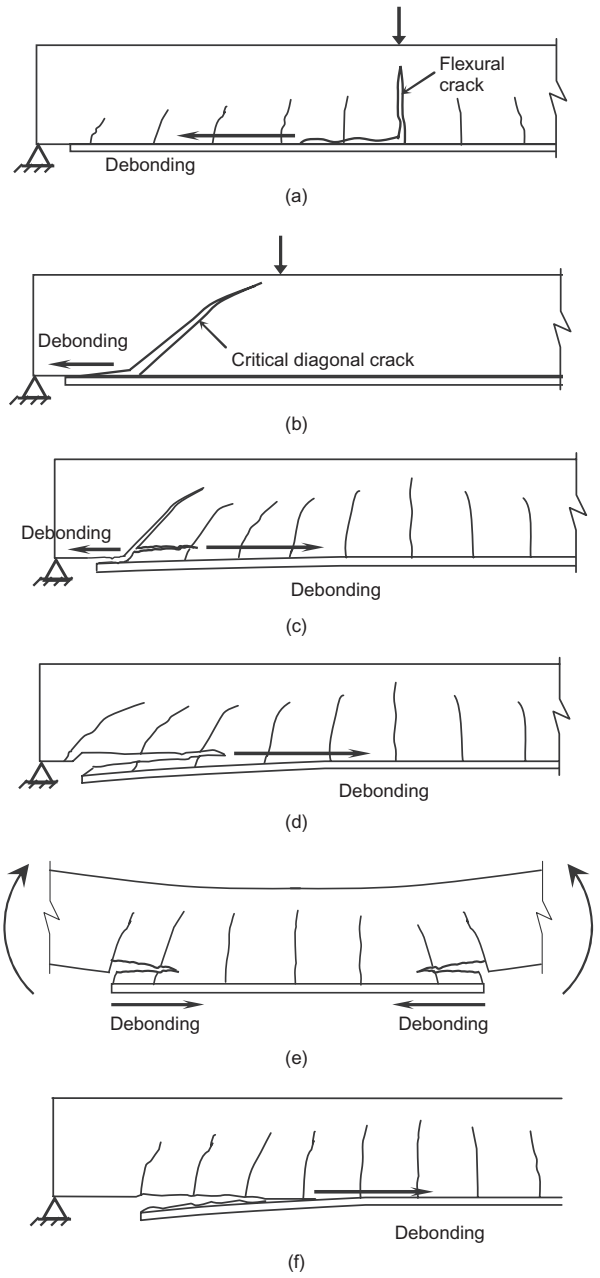

Figure 8. Debonding failure modes of RC beams bonded with a soffit FRP plate: (a) IC debonding; (b) CDC debonding; (c) CDC debonding with concrete with separation; (d) concrete cover separation; (e) concrete cover separation under pure bending; (f) plate end interfacial debonding

(*a*) critical diagonal crack (CDC) debonding (Figure 8(b))[23]
(*b*) CDC debonding with concrete cover separation (Figure 8(c))[8]
(*c*) concrete cover separation (Figures 8(e) and 8(d))[1]
(*d*) plate end interfacial debonding (Figure 8(f)).[1] Based on the understanding gained from the existing studies, a simple description is given below for each of the distinct debonding failure modes.

5.2. IC debonding

When a major flexural or flexural-shear crack is formed in the concrete, the need to accommodate the large local strain concentration at the crack leads to immediate but very localised debonding of the FRP plate from the concrete in the close vicinity of the crack, but this localised debonding is not yet able to propagate. The tensile stresses released by the cracked concrete are transferred to the FRP plate and steel rebars, so high local interfacial stresses between the FRP plate and the concrete are induced near the crack. As the applied loading further increases, the tensile stresses in the plate and hence the interfacial stresses between the FRP plate and the concrete near the crack also increase. When these stresses reach critical values, debonding starts to propagate towards one of the plate ends, generally the nearer end where the stress gradient in the plate is higher.

A typical picture of flexural crack-induced debonding is shown in Figure 9, which shows that a thin layer of concrete remained attached to the plate suggesting that failure occurred in the concrete adjacent to the adhesive-to-concrete interface. IC debonding failures are more likely to occur in shallow beams. This is because shallow beams are more prone to flexural cracking which leads to IC debonding, and less prone to shear cracking which is associated with plate end debonding. In general, IC debonding failures are more ductile than plate end debonding failures.

5.3. Concrete cover separation

Concrete cover separation involves crack propagation along the level of the steel tension reinforcement. Failure of the concrete cover is initiated by the formation of a crack near the plate end. The crack propagates to and then along the level of the steel tension reinforcement, resulting in the separation of the concrete cover. As the failure occurs away from the bondline, this is not a debonding failure mode in strict terms, although it is closely associated with stress concentration near the ends of the bonded plate. A typical picture of a cover separation failure is shown in Figure 10. The cover separation failure mode is a rather brittle failure mode.

5.4. Plate-end interfacial debonding

A debonding failure of this form is initiated by high interfacial shear and normal stresses near the end of the plate that exceed the strength of the weakest element, generally the concrete. Debonding initiates at the plate end and propagates towards the middle of the beam (Figure 8(f) and Figure 11). This failure mode is only likely to occur when the plate is significantly narrower than the beam section, as otherwise, failure tends to be by concrete cover separation (i.e. the steel bars–concrete interface controls the failure instead).

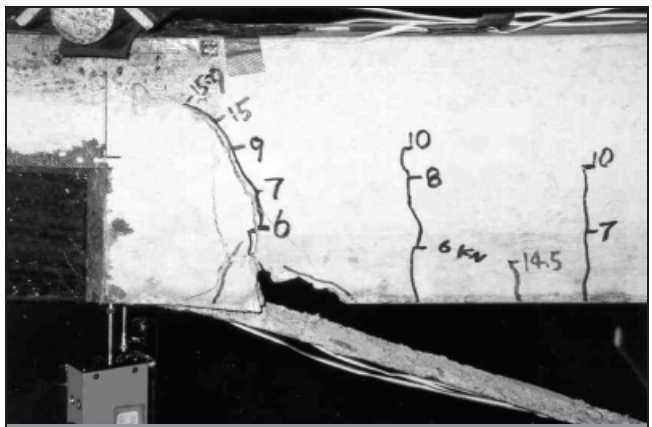

Figure 9. FRP-plated RC beam: IC debonding

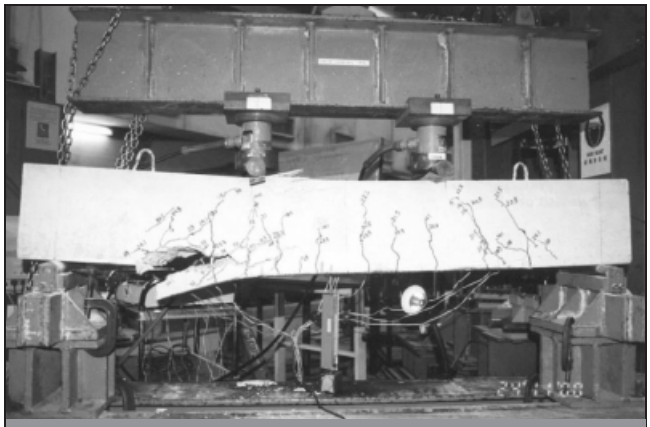

Figure 10. FRP-plated RC beam: concrete cover separation

Figure 11. FRP-plated RC beam: plate end interfacial debonding

5.5. CDC debonding

This mode of debonding failure occurs in flexurally strengthened beams where the plate end is located in a zone of high shear force but low moment (e.g. a plate end near the support of a simply supported beam) and the amount of steel shear reinforcement is limited. In such beams, a major diagonal shear crack (critical diagonal crack, or CDC) forms and intersects the FRP plate, generally near the plate end. As the crack widens, high interfacial stresses between the plate and the concrete are induced, leading to the eventual failure of the beam by debonding of the plate from the concrete; the debonding crack propagates from the CDC towards the plate end (Figure 12).

In a beam with a larger amount of steel shear reinforcement, multiple shear cracks of smaller widths instead of a single major shear crack dominate the behaviour, so CDC debonding is much less likely. Instead, cover separation takes over as the controlling debonding failure mode. In other cases, particularly when the plate end is very close to the zero-moment location, CDC debonding leads only to the local detachment of the plate end, but the beam is able to resist higher loads until cover separation occurs (Figure 8(c)). The local detachment owing to CDC debonding effectively moves the plate end to a new location with a larger moment, and cover separation then starts from this 'new end'. The CDC failure mode is thus related to the

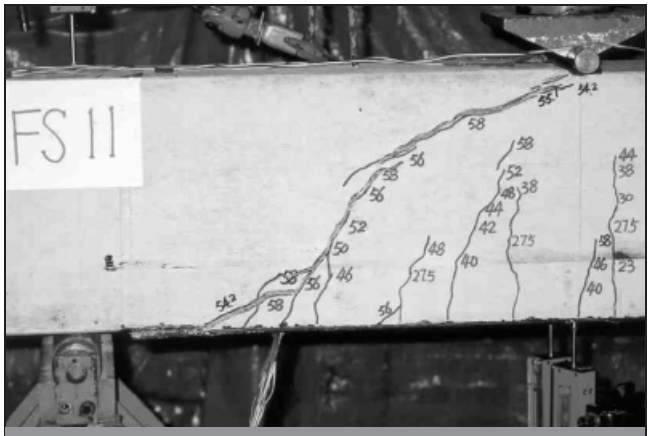

Figure 12. FRP-plated RC beam: CDC debonding

cover separation failure mode. If a flexurally strengthened beam is also shear-strengthened with U-jackets to ensure that the shear strength remains greater than the flexural strength, the CDC debonding failure mode may be effectively suppressed.

6. DEBONDING FAILURE MODES OF SHEAR-STRENGTHENED RC BEAMS

The shear failure process of FRP-strengthened RC beams involves the development of either a single major diagonal shear crack or a number of diagonal shear cracks, similar to normal RC beams without FRP strengthening.[9,10] For ease of description, the existence of a single major diagonal shear crack (the critical shear crack) is assumed whenever necessary. This treatment is conservative because recent research has shown that the existence of multiple cracks is beneficial for the development of the maximum debonding stress in the FRP.[26,27] Eventual failure of almost all test beams occurred in one of the two main failure modes: tensile rupture of the FRP and debonding of the FRP from the concrete. The FRP rupture failure mode has been observed in almost all tests on beams with complete FRP wraps and in some tests on beams with FRP U-jackets, while the debonding failure mode has been observed in almost all tests on beams with FRP side strips and most tests on beams with FRP U-jackets. Generally, both failure modes start with a debonding propagation process from the critical shear crack. Tensile rupture starts in the most highly stressed FRP strip, followed rapidly by the rupture of other FRP strips intersected by the critical shear crack. In beams with complete FRP wraps, it is also common that many of the FRP strips intersected by the critical shear crack have debonded from the sides over the full height of the beam before tensile rupture failure occurs. In beams whose failure is by debonding of the FRP from the RC beam, failure involves a process of sequential debonding of FRP strips starting from the most vulnerable strip (Figure 13).

7. OTHER ASPECTS OF DEBONDING

The risk of debonding is increased by a number of factors associated with the quality of on-site application. These include poor workmanship and the use of inferior adhesives. The effects of these factors can be minimised if due care is exercised in the application process to ensure that debonding failure is controlled by concrete. In addition, small unevenness of the concrete surface may cause localised debonding of the FRP plate but it is unlikely that such small unevenness can lead to the complete separation of the FRP plate from the

Figure 13. FRP-plated RC beams: debonding of FRP U-jackets

concrete member. Mechanical anchors and FRP U-jackets can be used in soffit plated beams to prevent plate end debonding. The latter may be used for shear strengthening at the same time. For beams shear strengthened with FRP U-jackets and side strips, mechanical anchors can also be used to suppress FRP debonding failure so that the failure mode is changed from debonding to rupture. However, care needs to be excised to avoid local failure adjacent to the anchors.

8. DEBONDING STRENGTH MODELS FOR FLEXURALLY STRENGTHENED RC BEAMS

8.1. Plate end debonding

Many factors control the likeliness of a particular plate end debonding failure mode for a given plated RC beam. For example, for an RC beam with a relatively low level of internal steel shear reinforcement, each of the plate end debonding modes (Figure 8) may become critical when the plate length or width is varied. When the distance between a plate end and the adjacent beam support (plate end distance) is very small, a CDC may form, causing a CDC debonding failure of the beam (Figure 8(b)). If the plate end distance is increased, the CDC may fall outside the plated region, and only concrete cover separation is observed (Figure 8(d)). Between these two modes, CDC debonding followed by concrete cover separation (Figure 8(c)) may occur; this mode is critical if the CDC debonding failure load is lower than the shear resistance of the original RC beam as well as the cover separation failure load so that the load can still be increased following CDC debonding. As the plate end moves further away from the support, the cover separation mode remains the controlling mode, and the plate end crack that appears prior to crack propagation along the level of steel tension reinforcement becomes increasingly vertical.[3] For the extreme case of a plate end in the pure bending region, the plate end crack is basically vertical (Figure 8(e)). For any given plate end position, if the plate width is sufficiently small compared with that of the RC beam, the interface between the soffit plate and the RC beam becomes a more critical plane than the interface between the steel tension bars and the concrete, and plate end interfacial debonding (Figure 8(f)) becomes the critical mode. However, this mode rarely occurs when the RC beam and the bonded plate have similar widths.

Given the large variety of parameters that govern plate end debonding failures, the development of a reliable strength model is not a simple task. The recent model by Teng and Yao[28] is the only model that appears to cover all the variations in plate end debonding failure modes. The model caters for any combination of plate end moment and shear force by way of the following interaction curve

$$\left(\frac{V_{\mathrm{db,end}}}{V_{\mathrm{db,s}}}\right)^2+\left(\frac{M_{\mathrm{db,end}}}{M_{\mathrm{db,f}}}\right)^2=1{\cdot}0 \tag{7}$$

where $V_{\mathrm{db,end}}$ and $M_{\mathrm{db,end}}$ are the plate end shear force and the plate end moment at debonding respectively, $M_{\mathrm{db,f}}$ is the flexural debonding moment when the beam section at the plate end is not subjected to any shear force (i.e. within the constant bending moment region) and $V_{\mathrm{db,s}}$ is the shear debonding force when the beam section at the plate end is not subjected to any bending moment (e.g. at the supports in a simply supported beam).

The flexural debonding moment, which is the bending moment that causes debonding of a plate end located in the pure bending zone of a beam, is found from

$$M_{\mathrm{db,f}}=\frac{0{\cdot}488\,M_{\mathrm{u,0}}}{(\alpha_{\mathrm{flex}}\alpha_{\mathrm{axial}}\alpha_{\mathrm{w}})^{1/9}}\leqslant M_{\mathrm{u,0}} \tag{8}$$

where α_{flex}, α_{axial} and α_{w} are three dimensionless parameters defined by

$$\alpha_{\mathrm{flex}}=\left[\left((EI)_{\mathrm{c,frp}}\right)-\left((EI)_{\mathrm{c,0}}\right)\right]/\left((EI)_{\mathrm{c,0}}\right) \tag{9a}$$

$$\alpha_{\mathrm{axial}}=E_{\mathrm{frp}}\,t_{\mathrm{frp}}/(E_{\mathrm{c}}d) \tag{9b}$$

$$\alpha_{\mathrm{w}}=b_{\mathrm{c}}/b_{\mathrm{frp}},\qquad b_{\mathrm{c}}/b_{\mathrm{frp}}\leqslant 3 \tag{9c}$$

where $(EI)_{\mathrm{c,frp}}$ and $(EI)_{\mathrm{c,0}}$ are the flexural stiffnesses of the cracked section with and without an FRP plate respectively; $E_{\mathrm{frp}}t_{\mathrm{frp}}$ is the axial rigidity per unit width of the FRP plate; E_{c} is the elastic modulus of concrete, b_{c} and d are the width and effective depth of the RC beam respectively; and $M_{\mathrm{u,0}}$ is the theoretical ultimate moment of the unplated section which is also the upper bound of the flexural debonding moment $M_{\mathrm{db,f}}$.

The shear debonding force $V_{\mathrm{db,s}}$, which is the shear force causing debonding of a plate end located in a region of (nearly) zero moment, can be found from

$$V_{\mathrm{db,s}}=V_{\mathrm{c}}+\varepsilon_{\mathrm{v,e}}\overline{V_{\mathrm{s}}}\qquad\text{with}\qquad\varepsilon_{\mathrm{v,e}}\leqslant\varepsilon_{\mathrm{y}}=\frac{f_{\mathrm{y}}}{E_{\mathrm{s}}} \tag{10}$$

where V_{c} and $\varepsilon_{\mathrm{v,e}}\overline{V_{\mathrm{s}}}$ are the contributions of the concrete and the internal steel shear reinforcement to the shear capacity of the beam respectively, and $\overline{V_{\mathrm{s}}}$ is the shear force carried by the steel shear reinforcement per unit strain, that is

$$\overline{V_{\mathrm{s}}}=A_{\mathrm{sv}}E_{\mathrm{sv}}d_{\mathrm{e}}/s_{\mathrm{v}} \tag{11}$$

where A_{sv}, E_{sv} and s_v are the total cross-sectional area of the two legs of each stirrup, the elastic modulus and the longitudinal spacing of the stirrups respectively. In Equation 10, $\varepsilon_{v,e}$ is the strain in the steel shear reinforcement, referred to here as the effective strain, and this effective strain may be well below the yield strain of the steel shear reinforcement ε_y. It should be noted that the bonded soffit plate also makes a small contribution to the shear debonding force $V_{db,s}$ but this contribution is small and is ignored in this debonding strength model.

Based on available test results, Teng and Yao[28] proposed that

$$\varepsilon_{v,e} = \frac{10}{(\alpha_{flex}\alpha_E\alpha_t\alpha_w)^{1/2}} \quad (12)$$

where α_{flex} and α_w are given by Equations 9a and c respectively, while the other two dimensionless parameters are defined by

$$\alpha_E = E_{frp}/E_c \quad (13a)$$

and

$$\alpha_t = (t_{frp}/d)^{1\cdot3} \quad (13b)$$

For the prediction of V_c in design, the design formula in any national code may be used.

8.2. IC debonding

Two simple and reliable IC debonding strength models have been developed by Teng *et al.*[24] and Lu *et al.*[7] The first model[24] is a simple modification of the bond strength model developed by Chen and Teng.[16] Lu *et al.*'s model[7] is based on the results of an extensive finite element study in which the simplified bond–slip model of Lu *et al.*[20] was used. Chen *et al.*[25] explored an alternative approach that is based on rigorous analytical work on the behaviour of the FRP-to-concrete interfaces between two adjacent cracks.[26,27] Chen *et al.*'s approach[25] therefore has the most sound mechanics basis and is more versatile (e.g. it is applicable to all loading conditions). Preliminary research presented in Chen *et al.*[25] has shown this model to be promising, and further work is in progress.

All the three models mentioned above predict a stress or strain value in the FRP plate at which IC debonding is expected to occur. According to Lu *et al.*'s model,[7] this debonding stress is given by

$$\sigma_{dbic} = 0\cdot114(4\cdot41 - \alpha)\tau_{max}\sqrt{\frac{E_{frp}}{t_{frp}}} \quad (14)$$

$$\tau_{max} = 1\cdot5\beta_w f_t \quad (15a)$$

$$\alpha = 3\cdot41 L_{ee}/L_d \quad (15b)$$

where L_d (mm) is the distance from the loaded section to the end of the FRP plate while L_{ee} (mm) is given by

$$L_{ee} = 0\cdot228\sqrt{E_{frp}\,t_{frp}} \quad (16)$$

Again, Lu *et al.*[7] adopted a slightly different expression from that defined by Equation 2 for the width ratio factor β_w, but the expression given by Equation 2 can be used in this model without any significant loss of accuracy.

9. DEBONDING STRENGTH MODELS FOR SHEAR-STRENGTHENED RC BEAMS

Several approaches have been used to predict the shear strength of FRP-strengthened RC beams. These include the modified shear friction method, the compression field theory, various truss models and the design code approach.[29] The vast majority of existing research has, however, adopted the design code approach that is discussed below. The total shear resistance of FRP-strengthened RC beams in this approach is commonly assumed to be equal to the sum of the three components from concrete, internal steel shear reinforcement and external FRP shear reinforcement respectively. Consequently, the shear strength of an FRP-strengthened beam V_u is given in the following form

$$V_u = V_c + V_s + V_{frp} \quad (17)$$

where V_c is the contribution of concrete, V_s is the contribution of steel stirrups and bent-up bars and V_{frp} is the contribution of FRP. V_c and V_s may be calculated according to provisions in existing design codes. The contribution of FRP is found by truss analogy, similar to the determination of the contribution of steel shear reinforcement. Two parameters are important in determining the FRP contribution: the shear crack angle which is generally assumed to be 45° for design use and the average stress (or effective stress) in the FRP strips intersected by the critical shear crack. Different models differ mainly in the definition of this effective stress. It may be noted that the design code approach neglects the interactions between the external FRP and internal steel stirrups and concrete. The validity of this assumption has been questioned by several researchers,[1,30–32] but the approach is the least involved for design, most mature and appears to be conservative for design in general. The most advanced model for FRP debonding failure following the design code approach is probably that developed by Chen and Teng,[10] which employed an accurate bond strength model,[16] leading to accurate predictions.

According to Chen and Teng,[10] the contribution of the FRP to the shear strength of the RC beam for a general strengthening scheme with FRP strips of the same width bonded on both sides of the beam (Figure 14) and with an assumed critical shear crack angle of $\theta = 45°$, is given by

$$V_{frp} = 2f_{frp,e}\,t_{frp}\,w_{frp}\frac{h_{frp,e}(\sin\beta + \cos\beta)}{s_{frp}} \quad (18)$$

where $f_{frp,e}$ is the average stress of the FRP intersected by the shear crack at the ultimate limit state, w_{frp} is the width of each

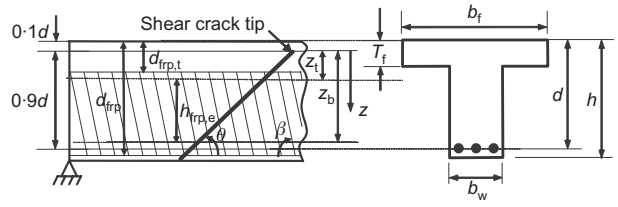

Figure 14. A general shear strengthening scheme

individual FRP strip (perpendicular to the fibre orientation), s_{frp} is the horizontal spacing of FRP strips (i.e. the centre-to-centre distance of FRP strips along the longitudinal axis of the beam), β is the angle of the inclination of fibres in the FRP to the longitudinal axis of the beam (measured clockwise for the left side of the beam as shown in Figure 2), and $h_{frp,e}$ is the effective height of the FRP bonded on the web

$$h_{frp,e} = z_b - z_t \tag{19}$$

where z_t and z_b are the coordinates of the top and the bottom ends of the effective FRP (Figure 14)

$$z_t = d_{frp,t} \tag{20a}$$

$$z_b = 0{\cdot}9d - (h - d_{frp}) \tag{20b}$$

in which $d_{frp,t}$ is the distance from the compression face to the top end of the FRP (thus $d_{frp,t} = 0$ for complete wrapping), h is the height of the beam and d_{frp} is the distance from the compression face to the lower end of the FRP. When FRP is bonded to the full height of the beam sides, Equation 19 reduces to $h_{frp,e} = 0{\cdot}9d$ as $z_t = 0$ and $z_b = 0{\cdot}9d$.

The FRP stress distribution at debonding failure is non-uniform chiefly because the bond lengths of the FRP strips vary with the vertical position of the critical shear crack at a given section. Chen and Teng[10] expressed the average (or effective) stress in the FRP along the critical crack $f_{frp,e}$ at the ultimate limit state as

$$f_{frp,e} = D_{frp}\sigma_{frp,max} \tag{21}$$

in which $\sigma_{frp,max}$ is the maximum stress that can be reached in the FRP intersected by the critical shear crack and D_{frp} is the stress distribution factor

$$\sigma_{frp,max} = \min\left\{ f_{frp},\ \alpha\beta_w\beta_L\sqrt{\frac{E_{frp}}{t_{frp}}\sqrt{f'_c}} \right. \tag{22}$$

$$D_{frp} = \begin{cases} \dfrac{2}{\pi\lambda}\dfrac{1-\cos(\pi\lambda/2)}{\sin(\pi\lambda/2)} & \text{if } \lambda \leqslant 1 \\ 1 - \dfrac{\pi - 2}{\pi\lambda} & \text{if } \lambda > 1 \end{cases} \tag{23}$$

where the coefficient α has the best fit value of 0·427 and the 95 percentile characteristic value of 0·315 for design based on Chen and Teng's bond strength model,[16] and β_L and β_w are as defined by Equations 2 and 3. For a shear strengthened beam with the fibres being at an angle β to the longitudinal axis of the beam, the expressions for β_L and β_w are re-written as

$$\beta_L = \begin{cases} 1 & \text{if } \lambda \geqslant 1 \\ \sin\dfrac{\pi\lambda}{2} & \text{if } \lambda < 1 \end{cases} \tag{24a}$$

$$\beta_w = \sqrt{\frac{2 - (w_{frp}/s_{frp}\sin\beta)}{1 + (w_{frp}/s_{frp}\sin\beta)}} \geqslant \frac{\sqrt{2}}{2} \tag{24b}$$

Note that $w_{frp}/(s_{frp}\sin\beta)$ is less than 1 for FRP strips with gaps. It becomes 1 when no gap exists between FRP strips and for continuous sheets or plates, yielding the lower limit value of $\sqrt{2}/2$ for β_w. The normalised maximum bond length λ and the maximum bond length L_{max} of the FRP strips are given by

$$\lambda = \frac{L_{max}}{L_e} \tag{25a}$$

$$L_{max} = \begin{cases} \dfrac{h_{frp,e}}{\sin\beta} & \text{for U jackets} \\ \dfrac{h_{frp,e}}{2\sin\beta} & \text{for side plates} \end{cases} \tag{25b}$$

where the effective bond length L_e of the FRP strips is defined by Equation 4. The number 2 appears in the denominator for side plates in Equation 25b because the FRP strip with the maximum bond length appears at the lower end of the critical shear crack for U-jacketing but at the middle for side bonding. Equation 23 is applicable to both U-jackets and side strips. The actual calculated values are different for these two cases even if the configuration of the bonded FRP is the same on the beam sides because the maximum bond length L_{max} for U-jackets is twice that for side strips (see Equation 25b).

10. CONCLUDING REMARKS

This paper has been concerned with the mechanics of debonding failures in RC beams strengthened in either flexure or shear with externally bonded FRP reinforcement. A systematic classification of possible debonding failure modes has been presented. The mechanisms and processes of the different debonding failure modes have been examined. Furthermore, advanced strength models for the key debonding failure modes have been summarised. The information presented in this paper may be directly applied in the practical design of FRP strengthening systems for RC beams and serve as a useful basis for the future development of design provisions in design codes and guidelines.

Despite the extensive existing research, many issues remain to be clarified. Within the context of monotonic loading and short-term behaviour, the existing theoretical debonding strength models require further improvements and the effects of preloading, load distributions, pre-tensioning of the FRP plate, and anchorage measures require a great deal of further research. Beyond the confinement of monotonic loading and short-term behaviour, major issues that call for further research include debonding under cyclic and dynamic loading as well as long-term durability.

ACKNOWLEDGEMENTS

The authors are indebted to their students, assistants and collaborators for their contributions to the research summarised here. They would also gratefully like to acknowledge the financial support provided by the Research Grants Council of the Hong Kong Special Administrative Region, The Hong Kong Polytechnic University, the Natural Science Foundation of China, the Scottish Funding Council for the Joint Research Institute between the University of Edinburgh and Heriot-Watt University, which forms part of the Edinburgh Research Partnership in Engineering and Mathematics (ERPem) and the Royal Society in the UK.

This paper was originally presented at the International Conference on Structures and Granular Solids: from Scientific Principles to Engineering Applications held in honour of Professor J. Michael Rotter of the University of Edinburgh (Chen J. F., Ooi J. Y. and Teng J. G. (eds). Structures and granular solids: from scientific principles to engineering applications. *Proceedings of the International Conference in Celebration of the 60th Birthday of Professor J. Michael Rotter*, CRC Press/Balkema). The authors would like to thank the publisher of the conference proceedings, CRC Press/Balkema of the Taylor and Francis Group, London, UK, for permission to include the paper in this special issue.

REFERENCES

1. Teng J. G., Chen J. F., Smith S. T. and Lam L. *FRP-Strengthened RC Structures*. Wiley, Chichester, 2002.
2. Hollaway L. C. and Teng J. G. (eds). *Strengthening and Rehabilitation of Civil Infrastructures Using FRP Composites*. Woodhead Publishing Limited, Cambridge, 2008.
3. Smith S. T. and Teng J. G. Shear-bending interaction in debonding failures of FRP-plated RC beams. *Advances in Structural Engineering,* 2003, **6**, No. 3, 183–199.
4. Teng J. G., Lam L., Chan W. and Wang J. S. Retrofitting of deficient RC cantilever slabs using GFRP strips. *Journal of Composites for Construction, ASCE*, 2000, **4**, No. 2, 75–84.
5. Smith S. T. and Teng J. G. FRP-strengthened RC beams-I: Review of debonding strength models. *Engineering Structures,* 2002, **24**, No. 4, 385–395.
6. Smith S. T. and Teng J. G. FRP-strengthened RC structures. II: Assessment of debonding strength models. *Engineering Structures,* 2002, **24**, No. 4, 397–417.
7. Lu X. Z., Teng J. G., Ye L. P and Jiang J. J. Intermediate crack debonding in FRP-strengthened RC beams: FE analysis and strength model. *Journal of Composites for Construction, ASCE*, 2007, **11**, No. 2, 161–174.
8. Yao J. and Teng J. G. Plate end debonding in FRP-plated RC beams-I: experiments. *Engineering Structures*, 2007, **29**, No. 10, 2457–2471.
9. Chen J. F. and Teng J. G. Shear capacity of FRP strengthened RC beams: FRP rupture. *Journal of Structural Engineering, ASCE*, 2003, **129**, No. 5, 615–625.
10. Chen J. F. and Teng J. G. Shear capacity of FRP strengthened RC beams: FRP debonding. *Construction and Building Materials*, 2003, **17**, No. 1, 27–41.
11. Cao S. Y., Chen J. F., Teng J. G., Hao Z. and Chen J. Debonding in RC beams shear strengthened with complete FRP wraps. *Journal of Composites for Construction, ASCE*, 2005, **9**, No. 5, 417–428.
12. Smith S. T. and Teng J. G. Interfacial stresses in plated beams. *Engineering Structures*, 2001, **23**, No. 7, 857–871.
13. Teng J. G., Zhang J. W. and Smith S. T. Interfacial stresses in RC beams bonded with a soffit plate: a finite element study. *Construction and Building Materials,* 2002, **16**, No. 1, 1–14.
14. Shen H. S., Teng J. G. and Yang J. Interfacial stresses in beams and slabs bonded with a thin plate. *Journal of Engineering Mechanics, ASCE*, 2001, **127**, No. 4, 399–406.
15. Yang J., Teng J. G. and Chen J. F. Interfacial stresses in soffit-plated reinforced concrete beams. *Proceedings of the Institution of Civil Engineers, Structures and Buildings*, 2004, **157**, No. SB1, 77–89.
16. Chen J. F. and Teng J. G. Anchorage strength models for FRP and steel plates bonded to concrete. *Journal of Structural Engineering, ASCE*, 2001, **127**, No. 7, 784–791.
17. Yuan H., Teng J. G., Seracino R., Wu Z. S. and Yao J. Full-range behavior of FRP-to-concrete bonded joints. *Engineering Structures,* 2004, **26**, No. 5, 553–565.
18. Yao J., Teng J. G. and Chen J. F. Experimental study on FRP-to-concrete bonded joints. *Composites-Part B: Engineering*, 2005, **36**, No. 2, 99–113.
19. Chen J. F., Yang Z. J. and Holt G. D. FRP or steel plate-to-concrete bonded joints: effect of test methods on experimental bond strength. *Steel and Composite Structures: An International Journal,* 2001, **1**, No. 2, 231–244.
20. Lu X. Z., Teng J. G., Ye L. P and Jiang J. J. Bond–slip models for FRP sheets/plates bonded to concrete. *Engineering Structures*, 2005, **27**, No. 6, 920–937.
21. Lu X. Z., Ye L. P., Teng J. G. and Jiang J. J. Meso-scale finite element model for FRP sheets/plates bonded to concrete. *Engineering Structures*, 2005, **27**, No. 4, 564–575.
22. Buyukozturk O., Gunes O. and Karaca E. Progress on understanding debonding problems in reinforced concrete and steel members strengthened using FRP composites. *Construction and Building Materials*, 2004, **18**, No. 11, 9–19.
23. Oehlers D. J. and Seracino R. *Design of FRP and Steel Plated RC Structures: Retrofitting Beams and Slabs for Strength, Stiffness and Ductility*. Elsevier, Oxford, 2004.
24. Teng J. G., Smith S. T., Yao J. and Chen J. F. Intermediate crack induced debonding in RC beams and slabs. *Construction and Building Materials*, 2003, **17**, No. 6 and 7, 447–462.
25. Chen J. F., Teng J. G. and Yao J. Strength model for intermediate crack debonding in FRP-strengthened concrete members considering adjacent crack interaction. *Proceedings of 3rd International Conference on FRP Composites in Civil Engineering (CICE 2006), Miami*, 2006, 67–70.

26. TENG J. G., YUAN H. and CHEN J. F. FRP-to-concrete interfaces between two adjacent cracks: theoretical model for debonding failure. *International Journal of Solids and Structures*, 2006, **43**, No. 18–19, 5750–5778.
27. CHEN J. F., YUAN H. and TENG J. G. Debonding failure along a softening FRP-to-concrete interface between two adjacent cracks in concrete members. *Engineering Structures*, 2007, **29**, No. 2, 259–270.
28. TENG J. G. and YAO J. Plate end debonding in FRP-plated RC beams-II: strength model. *Engineering Structures*, 2007, **29**, No. 10, 2472–2486.
29. TENG J. G., LAM L. and CHEN J. F. Shear strengthening of RC beams using FRP composites. *Progress in Structural Engineering and Materials,* 2004, **6**, 173–184.
30. DENTON S. R., SHAVE J. D. and PORTER A. D. Shear strengthening of reinforced concrete structures using FRP composites. *Proceedings of the International Conference on Advanced Polymer Composites for Structural Applications in Construction*. Woodhead Publishing Limited, Cambridge, 2004, pp. 134–143.
31. QU Z., LU X. Z. and YE L. P. Size effect of shear contribution of externally bonded FRP U-Jackets for RC beams. *Proceedings of International Symposium on Bond Behaviour of FRP in Structures*. Hong Kong, 2005, pp. 371–379.
32. MOHAMED ASLI M. S., OEHLERS D. J. and SERACINO R. Vertical shear interaction model between external FRP transverse plates and internal steel stirrups. *Engineering Structures,* 2006, **28**, No. 3, 381–389.